Application of MEMS microphone array for acoustic holography

Zdeněk Havránek and Petr Beneš
Faculty of Electrical Eng. and Com., Brno University of Technology, Brno, Czech Republic.
Stanislav Klusáček
Central European Institute of Technology, Brno University of Technology, Brno, Czech Republic.

Summary
The paper shows the overall potential and applicability of microphone arrays equipped with MEMS miniature capacitive microphones for use with near-field acoustic holography algorithms to visualize and localize sound sources. Comprehensive test of double layer rectangular matrix microphone array and several acoustic holography algorithms has been carried out to find weaknesses of proposed MEMS array technology in practical measurement conditions including complex sources and disturbing sound field. Test setups include determination of secondary (disturbing) source strength, influence of distance of the primary and secondary sources and also measurement array stand-off distance on prediction accuracy of localization and characterization of sound and vibration sources. Attention is also focused on available signal-to-noise ratio of sound pressure measurement with applied MEMS microphones and its influence on determination of regularization parameters for inverse acoustic holography calculation. Drawbacks of complex or even unfeasible calibration procedure for such MEMS transducers also influence the presented prediction accuracy results in practical measurements.

PACS no. 43.60.Fg, 43.60.Sx, 43.60.Qv

1. Introduction

Analysis and visualization of radiated sound field from vibrating structures are necessary tasks for advanced vibration diagnostics and noise reduction. Localization and characterization of sound and vibration sources through acoustic measurement is one of the experimental procedures for fast evaluation of the current state of mechanical structures and components and are also applicable during design and development stage of cabins and enclosures in automotive or aircraft industry [1].

This paper focuses on analysis of applicability of simple hand-held measurement array equipped with the cheap MEMS microphones to localize and characterize sound sources using inverse approach using near-field acoustic holography methods. Near-field acoustic holography (NAH) formulates the procedures for forward estimation and also backward prediction of sound fields based on acoustic measurement in examined source near-field [2]. Preliminary analysis of applicability of a MEMS microphone array for acoustic holography has been already presented in the past [3]. In this paper more detailed analysis based on previous results has been carried out to eliminate some weaknesses included in previous results and provide more reliable and complex overview of applicability of this technology for localization of sound and vibration sources and analysis of radiated sound field from real structures in more realistic environmental conditions. This means usability of such measurement system in confined space where other disturbing sources or unwanted reflection are present. For practical usability it is also necessary to be able to estimate sound field near the examined source with the measurement array smaller that the source. Applicable calculation procedures for such experimental case are usually called "patch" holography methods and only these methods are of the interest in this research.

Methodology and technology discussed in this paper is limited to planar sources and to measurement procedures carried out with planar microphone arrays only. Specialized procedures applicable for non-planar (cylindrical, spherical) or even arbitrary geometries and usually based on finite or boundary elements are out of the scope of this paper.

2. Patch acoustic holography methods for confined space

For localization and characterization of sound sources in confined space it is necessary to use such procedures and algorithms which can distinguish between incoming and outgoing sound fields and thus they are able to successfully extract only that part of sound filed which is radiated from the source. Such methods need to adopt two parallel layers of acoustic sensors. In the easiest way these sensors measure only scalar acoustic variable - sound pressure. There are also vector sensors, like Microflown probe which can measure both sound pressure and acoustic particle velocity so they can directly evaluate vector of acoustic intensity in the examined sound field [4]. Measurements adopting vector sensors carry more information and in backward prediction (inverse calculation) of sound field near the sound source, they are less sensitive to noise and imperfections always included in the measured data [4]. Contrary these sensors are more expensive and large arrays equipped with such sensors are almost practically unusable due to their extreme price.

The most suitable calculation procedures for near-field acoustic holography which can adopt acoustic field information measured in two parallel planes and therefore called double or dual layer methods are an Equivalent Source Method (ESM) and the Statistically Optimized NAH algorithm (SONAH). ESM and SONAH avoid using transformation into wavenumber domain, thus eliminated leakage caused by windowing before DFT used in classical Fourier based algorithms [2]. In the next paragraphs only very general mathematical background of the above mentioned algorithms is presented. More detailed description can be found in literature.

1.1. Equivalent source method

Basic theory of the equivalent source method (ESM) is based on the assumption that sound field near the vibrating structure can be modelled by several number of simple sources placed inside the structure close to the radiating surface. Radiation of these simple sources (monopoles or dipoles) create sound field above the examined structure surface, so complete sound field is composed of superposition of these simple sources [5, 6]. For M measurement points on the hologram plane (number of microphones in the array) and N equivalent sources placed in the structure, the sound pressure vector $\boldsymbol{p}_{h1}$ measured in the acoustic near-field of the source on the one plane can be expressed by matrix form in equation 1.

$$\mathbf{p}_{\mathrm{h1}} = \mathrm{j}\rho\mathrm{ck}\mathbf{G}_1\mathbf{W}_1, \tag{1}$$

where ρ is the density of air, c is the speed of sound in air, k is the wave number and $\mathbf{W}_1$ is the column vector containing the strengths $w_{11}(\mathbf{r}_{o1})$, $w_{12}(\mathbf{r}_{o2})$, .. w_{1n} $(\mathbf{r}_{on})$ of the equivalent sources, $\mathbf{r}_{on}$ is the nth equivalent source location vector, and $\mathbf{G}_1$ is the transfer matrix between equivalent sources and the measurement points and is represented by Green's function in free space.

For this simple arrangement with only one measurement layer it is only needed to estimate source strengths $\mathbf{W}_1$ based on measured pressure field and then recalculate it to the requested positions very near the source surface as can be stated by equation 2.

$$\mathbf{p}_0 = \mathrm{j}\rho\mathrm{ck}\mathbf{G}_0\mathbf{W}_1, \tag{2}$$

When there could be other (disturbing) sound sources on the opposite side of the array, two measurement surfaces $\boldsymbol{p}_{h1}$ and $\boldsymbol{p}_{h2}$ are needed and also two fictitious surfaces S_1 and S_2 with the redistributed equivalent sources are necessary. Both incoming (superscript "i") and outgoing (superscript "o") sound fields are measured on the hologram planes. To estimate source strengths on the both sides of the measurement array several matrix equations can be written. Both directions of pressure field for the front hologram plane (closed to the examined source S_1) can be expressed by equation 3.

$$\mathbf{p}_{\mathrm{h1}} = \mathbf{p}_{\mathrm{h1}}^{\mathrm{i}} + \mathbf{p}_{\mathrm{h1}}^{\mathrm{o}}, \tag{3a}$$

$$\mathbf{p}_{\mathrm{h1}}^{\mathrm{o}} = \widetilde{\mathbf{G}}_1^{\mathrm{o}}\mathbf{W}_1,\ \mathbf{p}_{\mathrm{h1}}^{\mathrm{i}} = \widetilde{\mathbf{G}}_1^{\mathrm{i}}\mathbf{W}_2 \tag{3b}$$

Similarly for the rear hologram plane the equation 3 can be rewritten to equation 4.

$$\mathbf{p}_{\mathrm{h2}} = \mathbf{p}_{\mathrm{h2}}^{\mathrm{i}} + \mathbf{p}_{\mathrm{h2}}^{\mathrm{o}}, \tag{4a}$$

$$\mathbf{p}_{\mathrm{h2}}^{\mathrm{o}} = \widetilde{\mathbf{G}}_2^{\mathrm{o}}\mathbf{W}_1, \mathbf{p}_{\mathrm{h2}}^{\mathrm{i}} = \widetilde{\mathbf{G}}_2^{\mathrm{i}}\mathbf{W}_2 \tag{4b}$$

The source strengths vectors $\mathbf{W}_1$ and $\mathbf{W}_2$ can be estimated by combining equation 3 and 4.

$$\mathbf{W}_1 = \left(\widetilde{\mathbf{G}}_1^{\mathrm{o}} - \mathbf{Q}_1\widetilde{\mathbf{G}}_2^{\mathrm{o}}\right)^{\dagger}(\mathbf{p}_{\mathrm{h1}} - \mathbf{Q}_1\mathbf{p}_{\mathrm{h2}}),$$

$$\mathbf{W}_2 = \left(\widetilde{\mathbf{G}}_2^{\mathrm{i}} - \mathbf{Q}_2\widetilde{\mathbf{G}}_1^{\mathrm{i}}\right)^{\dagger}(\mathbf{p}_{\mathrm{h2}} - \mathbf{Q}_2\mathbf{p}_{\mathrm{h1}}), \tag{5}$$

where

$$\mathbf{Q}_1 = \widetilde{\mathbf{G}}_1^{\mathrm{i}}\left(\widetilde{\mathbf{G}}_2^{\mathrm{i}}\right)^{\dagger},\ \mathbf{Q}_2 = \widetilde{\mathbf{G}}_2^{\mathrm{o}}\left(\widetilde{\mathbf{G}}_1^{\mathrm{o}}\right)^{\dagger}. \quad (6)$$

Singular value decomposition can be used to calculate necessary matrix inversions (with superscript "†") in the above equations 5 and 6, where they are necessary for the case when the examined sound source with surface S_1 is totally absorbing. If there are any reflections from the surface S_1 one more calculation step is needed to estimate scattered field. The scattered field for totally reflecting surface S_1 can be expressed in matrix form with equation 7.

$$\mathbf{p}_{\mathrm{h1}}^{\mathrm{s}} = \widetilde{\mathbf{G}}_{1\mathrm{s}}^{\mathrm{o}}\mathbf{W}_2 \quad (7)$$

Radiated part of the examined source measured at the front hologram plane is calculated subtracting scattered field from the outgoing sound field as described by equation 8.

$$\mathbf{p}_{\mathrm{h1}}^{\mathrm{r}} = \mathbf{p}_{\mathrm{h1}}^{\mathrm{o}} - \mathbf{p}_{\mathrm{h1}}^{\mathrm{s}} = \widetilde{\mathbf{G}}_1^{\mathrm{o}}\mathbf{W}_1 - \widetilde{\mathbf{G}}_{1\mathrm{s}}^{\mathrm{o}}\mathbf{W}_2 \quad (8)$$

Finally it is necessary to estimate equivalent source strengths $\mathbf{W}_{\mathrm{r}}$ which represents only radiated part of the sound field comming from the examined source and this can be done by one last matrix inversion of the equation 9.

$$\mathbf{p}_{\mathrm{h1}}^{\mathrm{r}} = \widetilde{\mathbf{G}}_1^{\mathrm{r}}\mathbf{W}_{\mathrm{r}} \quad (9)$$

Complete derivation of Equivalent source method in noisy environment can be found in [7].

1.2. Statistically optimized NAH

This algorithm with acronym SONAH calculates forward or backward propagation directly in the spatial domain based on estimated set of elementary plane wave functions. These elementary plane wave functions Ψ_n, n = 1,2,..N, can describe the complete sound field near the examined source with equation 10.

$$\Psi_{\mathrm{n}}(\mathbf{r}) = \kappa\Phi_{\mathbf{k}_{\mathrm{n}}},$$
$$\Psi_{\mathrm{n}}(\mathbf{r}) \equiv \kappa F_n(k_z)\mathrm{e}^{j(k_x x + k_y y + k_z z)}, \quad (10)$$

where κ is a scaling factor for smoothing of wave spectra when regular sampling in the wave number domain is present. Amplitude weighting functions F_n have unit weighting at the virtual source plane. For complex estimation weights $\mathbf{c}(\mathbf{r})$ between the elementary wave set $\mathbf{A}$ of the sound field at the hologram plane and $\boldsymbol{\alpha}(\mathbf{r})$ at the estimation positions there can be written matrix relationship described by equation 11.

$$\mathbf{A}\mathbf{c}(\mathbf{r}) = \boldsymbol{\alpha}(\mathbf{r}) \quad (11)$$

Tikhonov regularized solution for $\mathbf{c}(\mathbf{r})$ can be then expressed by equation 12.

$$\mathbf{c}(\mathbf{r}) = \left(\mathbf{A}^{\mathrm{H}}\mathbf{A} + \varepsilon\mathbf{I}\right)^{-1}\mathbf{A}^{\mathrm{H}}\boldsymbol{\alpha}(\mathbf{r}), \quad (12)$$

where ε is a regularization parameter, $\mathbf{I}$ is a diagonal unity matrix and $\mathbf{A}^{\mathrm{H}}\mathbf{A}$ is the cross correlation matrix between the measurement points in the elementary wave functions domain and $\mathbf{A}^{\mathrm{H}}\boldsymbol{\alpha}(\mathbf{r})$ contains cross correlation between the measurement points and the estimation position $\mathbf{r}$. Complete derivation of both cross correlation matrices can be found in [8].

After evaluation of complex weights $\mathbf{c}(\mathbf{r})$ the sound pressure field at any point above examined source surface can be estimated with equation 13, where vector $\mathbf{p}$ contains measured (known) sound pressure values obtained at hologram plane.

$$\tilde{p}(\mathbf{r}) = \mathbf{p}^{\mathrm{T}}\mathbf{c}(\mathbf{r}) \quad (13)$$

To utilize also the secondary sources which can be present in confined space the SONAH algorithm can be extended to estimate incoming and outgoing sound field similarly as in ESM algorithm. Detailed derivation of the SONAH algorithm for non free-field conditions due to high complexity is not presented here and can be found in [8].

3. Experimental setup

Similarly to the study presented in [3] a reference sound source for generation of the radiating sound field above the planar structure was an thin plate with dimensions of 479x253 mm^2 and thickness of 2 mm made of aluminium alloy. The plate was placed on the soft foam with no edge clamping and was driven with harmonic point force by B&K electrodynamic shaker Type 4809 near one of the corners of the plate to successfully excite the most of its resonant frequencies. While the plate was unclamped (attached only to the shaker moving armature) it can be assumed as free-free. This vibrating surface produces significant sound field above its surface which has been used for evaluation of the measurement system equipped with double layer microphone array. To avoid any disturbances from any uncontrolled sound sources complete experimental setup has been placed in the small anechoic chamber with volume of approx. 10 m3 and satisfies free-field conditions from 250 Hz.

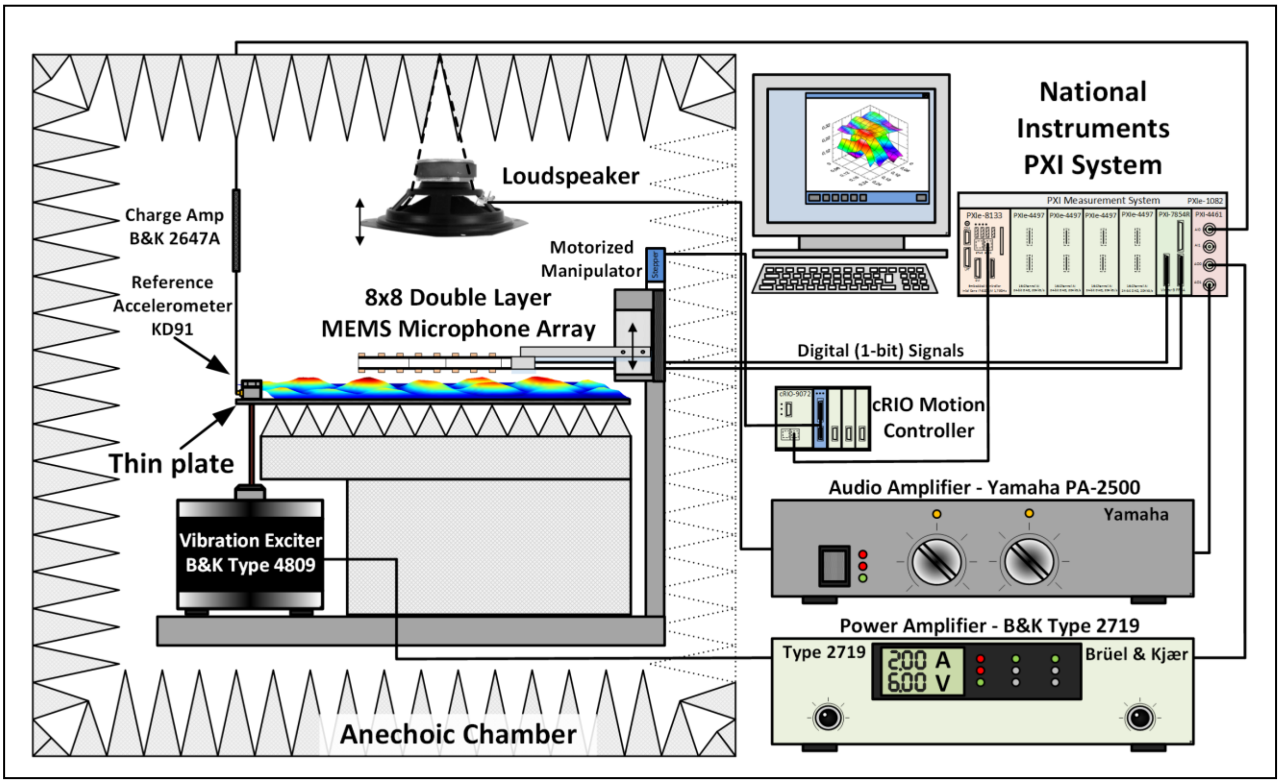

Figure 1. Sketch of the measurement setup for evaluation of double layer MEMS microphone array in small anechoic chamber.

Tested MEMS microphone array used for this experimental analysis and evaluation of this technology for practical usage was made of two layers of net dimensions of 210x210 mm^2 with microphone spacing of 30 mm which creates matrix of 8 by 8 microphones. The two parallel layers have a distance of also 30 mm. All these dimensions restrict usable frequency range up to approx. 5 kHz. The lower limit of this array depends on the processing algorithm and also on the measurement environment, where in this case it is down to 250 Hz (free field limit of the chamber). Microphone array was equipped with miniature commercial MEMS microphones SPM1437HM4H with digital PDM output manufactured by Knowles.

All digital signals from the microphones have been processed in real-time by FPGA programmable card PXI-7854R inside the National Instruments PXI system where all signal processing has been performed with software application programmed in LabVIEW. Implementation of acoustic holography algorithm has been made in Matlab.

On the figure 1, there can be seen complete measurement system installed in the small anechoic chamber. Real photography of the measurement setup is on the figure 2.

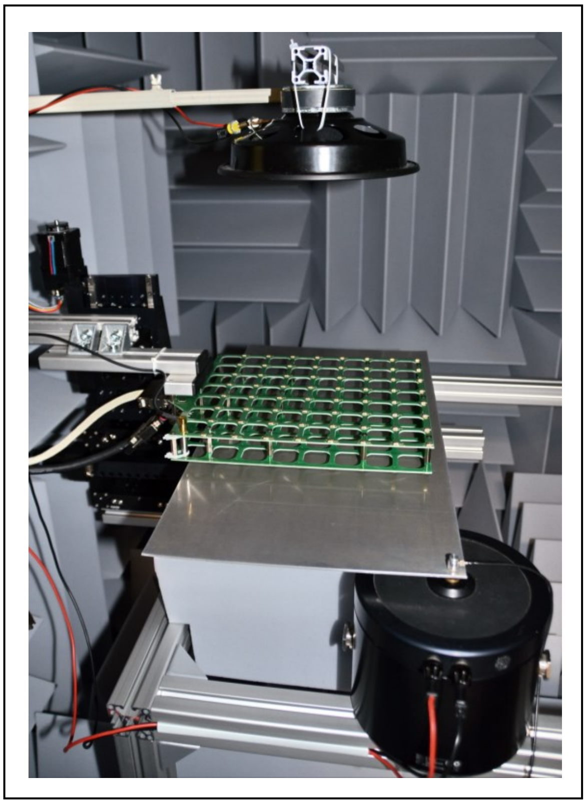

Figure 2. Photography of the measurement setup.

Microphone array has been mounted on the motorized manipulator to allow several stand-off distances from the primary source (thin plate). This motorized manipulator has been controlled by National Instruments cRIO platform and commanded through Ethernet interface from the same PXI system as the measurements. Similarly to the test case presented in [3] the radiated sound field coming from the aluminium plate can be disturbed with the secondary source which was represented by a loudspeaker mounted above the plate in two selected distances from the primary source (275 mm and 550 mm). To disturb primary sound field generated by the thin plate several magnitudes of driving voltage to the loudspeaker can be also selected.

4. Results and discussion

The comparison of prediction accuracies of both selected NAH algorithms have been based on measurement of **true** pressure field at calculation plane (10 mm and 30 mm) as a reference value and with consequent measurements in two parallel planes made in several stand-off distance from the plate surface (30/60 mm, 60/90 mm) as an input to the inverse holography calculation where **estimated** sound field in calculation plane has been obtained. For evaluation of the prediction accuracy in the whole patch area the error norm expressed with equation 14 has been used.

$$\mathrm{E_p} = 20\log\sqrt{\frac{\sum\left(|\mathbf{p}_x^{\mathrm{True}}|-|\tilde{\mathbf{p}}_x^{\mathrm{Estimated}}|\right)^2}{\sum|p_x^{\mathrm{True}}|^2}} \qquad (14)$$

First test case compares pressure prediction accuracy in free field conditions when disturbing source is turned off and for three combinations of stand-off and calculation distances. On the figure 3 there is presented prediction accuracy for ESM algorithm in single and dual layer version.

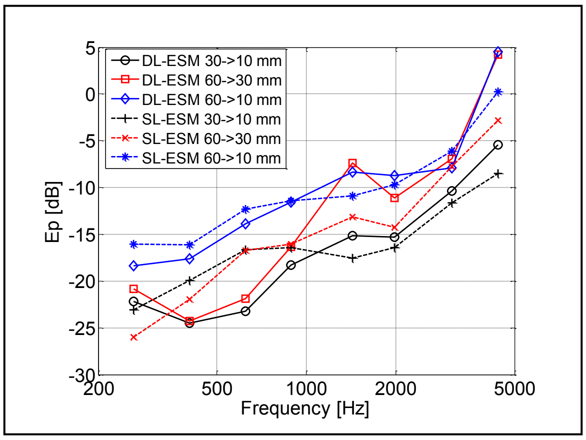

Figure 3. Comparison of prediction accuracy obtained with single and dual layer ESM method and three combinations of different stand-off and calculation plane distances.

It can be clearly seen that with increasing stand-off distance from the source surface, less evanescent components are captured and prediction accuracy decreases. Increasing of the error at higher frequencies is due to the scattering on the frame of the array, which can be seen more clearly in double layer calculation where this effect is more significant due to the utilization of rear layer information.

Next test case compares prediction accuracy again using ESM algorithm but with and without disturbing sound source. Results of this comparison are on the figure 4.

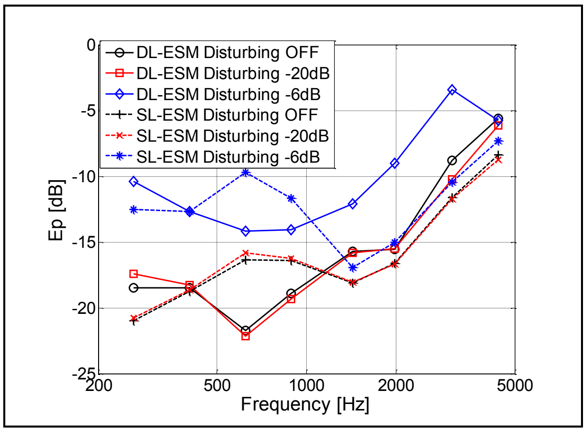

Figure 4. Comparison of prediction accuracy obtained with single and dual layer ESM method with recalculation from 30 mm to 10 mm and different strength of disturbing source (loudspeaker).

The results on the figure 4 show strong influence of the disturbing source to prediction accuracy of both single layer and dual layer ESM implementations while dual layer algorithm performs better in lower to mid-frequency range, where the accuracy improvement reaches 5 dB, but outside of this frequency range an information obtained from second layer deteriorates achieved accuracy which is due to its inaccuracy at high frequencies and there could be also some non-anechoic conditions at very low frequencies on the threshold of the free-field assumption of the chamber. Changing the expected position of the secondary (disturbing) source as a input parameter of parameter didn’t bring any improvement in the prediction accuracy. It can be also seen that strength of -20 dB of secondary source related to the strength of the primary source did not affect prediction accuracy significantly.

Third test case compares prediction accuracy using ESM and SONAH algorithm for measurements at 30/60 mm distance from the primary source (with prediction layer at 10 mm) and with two stand-off distances of disturbing source. Double layer SONAH algorithm performs better than single layer version also in low to mid-frequency band similarly as ESM. At higher frequencies above 2 kHz there are almost unnoticeable differences, but in compare with ESM, the SONAH algorithm performs with lower prediction error.

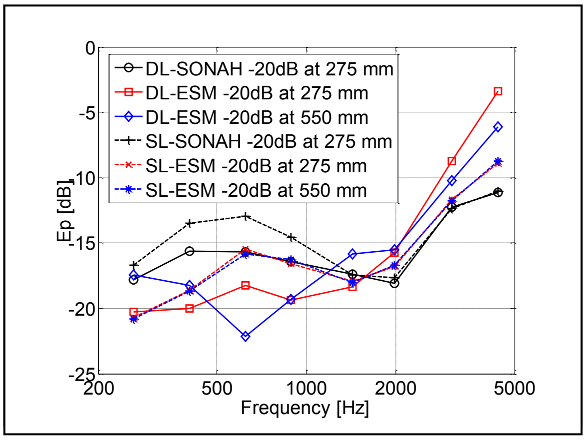

Figure 5. Comparison of prediction accuracy obtained with single and dual layer ESM and SONAH algorithms and for different disturbing source distance.

The last figure 6 shows sound pressure level spectrum obtained on one MEMS microphone during measurement of sound field radiated from thin plate driven at frequency of 625 Hz. It can be seen that noise floor in spectrogram is 60 dB below the radiated signal amplitude (the driving force for all test cases has been set to produce 1 mm/s vibration velocity at driving point).

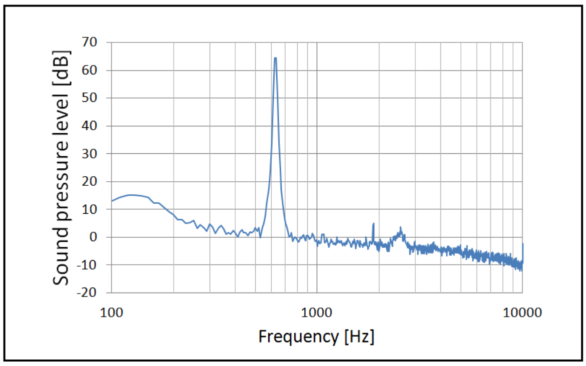

Figure 6. Sound pressure level spectrum measured with MEMS microphone above the radiating plate.

5. Conclusions

The MEMS rectangular microphone array accompanied with two patch acoustic holography algorithms have been tested for accuracy of radiated sound field prediction from the thin rectangular aluminium alloy plate. From all practical measurements it can be seen that prediction accuracy with measurements using MEMS microphone array and without strong disturbing source is very promising and achieve lower than -15 dB prediction error at frequency range up to 2 kHz. At higher frequencies, the influences of scattering on the array frame and inaccuracies in phase matching of the microphones lead to lower prediction accuracy. With secondary disturbing source present, the double layer algorithms performs better than single layer versions in ranges where measured data from rear layer are not considerably affected by transducers imperfections. Better prediction accuracy can be expected if precise phase calibration will be performed [9].

Acknowledgement

Authors gratefully acknowledge financial support from the Ministry of Education, Youth and Sports under projects No. LO1210 – „Energy for Sustainable Development (EN-PUR)" and CZ.1.07/2.3.00/30.0005 funded by European Regional Development Fund solved in the Centre for Research and Utilization of Renewable Energy, and grant No. FEKT-S-14-2429 - „The research of new control methods, measurement procedures and intelligent instruments in automation" financially supported by the internal science fund of Brno University of Technology.

References

[1] J. Hald, et all.: Measurement of absorption coefficient, surface admittance, radiated intensity and absorbed intensity on the panels of a vehicle cabin using a dual layer array with integrated position measurement. Proc. of SAE 2009.

[2] E.G. Williams: Fourier Acoustics: Sound radiation and Near-field Acoustical Holography. Academic Press, USA, 1999.

[3] Z. Havránek, P. Beneš, S. Klusáček: Comparison of patch acoustic holography methods for confined space. Proc. Inter-noise 2014, 1-10.

[4] E. Fernandez-Grande, F. Jacobsen, Q. Leclère: Sound field separation with sound pressure and particle velocity measurements. J. Acoust. Soc. Am. 132 (2012), 3818-3825.

[5] C.-X. Bi, X.-Z. Chen, J. Chen: Sound field separation technique based on equivalent source method and its application in nearfield acoustic holography. J. Acoust. Soc. Am. 123 (2008), 1472–1478.

[6] M. Pinho, J. Arruda: On the use of the equivalent source method for nearfield acoustic holography. ABCM Symposium Series in Mechatronics 1 (2004), 590-599.

[7] C.-X. Bi, J.S. Bolton: An equivalent source technique for recovering the free sound field in a noisy environment. J. Acoust. Soc. Am. 131 (2012), 1260-1270.

[8] J. Hald: Basic theory and properties of statistically optimized near-field acoustical holography. J. Acoust. Soc. Am. 125 (2009), 2105-2120.

[9] Z. Havránek, P. Beneš, S. Klusáček: Free-field calibration of MEMS microphone array used for acoustic holography. Proc. of ICSV 21, 2014, 1-8.